Jurnal Tribologi 40 (2024) 226-246

MYTRIBOS Malaysian Tribology Society

Jurnal Tribologi

Website : jurnaltribologi.mytribos.org e-issn: 2289-7232

Machining analysis of S45C carbon steel using finite element method

Jaharah A Ghani [1*], Muhammad Asyraf Ismanizan [1], Haniff Abdul Rahman [1], Che Hassan Che Haron [1], Afifah Zakiyyah Juri [1], Mohd. Shahir Kasim [2], Muhammad Rizal [3]

[1] Centre for Materials Engineering and Smart Manufacturing (MERCU), Department of Mechanical and Manufacturing Engineering, Universiti Kebangsaan Malaysia, MALAYSIA.
[2] Fakulti Reka Bentuk Inovatif dan Teknologi, Universiti Sultan Zainal Abidin, MALAYSIA.
[3] Department of Mechanical Engineering, Faculty of Engineering, Syiah Kuala University, INDONESIA.
[*]Corresponding author: jaharahaghani@ukm.edu.my

KEYWORDS

Finite element analysis
Turning process
Carbon steel S45C
Taguchi method

ABSTRACT

This study focuses on the application of the finite element method (FEM) in the machining of carbon steel bars S45C, which is widely used for producing machine structures, shafts, gears, and parts for actuators or sensors that commonly used in the automotive industry. The Abaqus CAE software has been utilized for the simulation study. The simulation was carried out according to the Taguchi L9 orthogonal array, with a cutting speed of 160 – 240 m/min, a feed rate of 0.1 – 0.4 mm/rev, and depth of cut of 0.15 – 0.35 mm. For comparison with the experiment, the parameters used in the industry were performed at a cutting speed of 200 m/min, a feed rate of 0.2 mm/rev, and depth of cut of 0.25 mm. The simulation results found that the optimal cutting parameters are at a cutting speed of 160 m/min, a depth of cut of 0.15 mm, and a feed rate of 0.1 mm/rev that resulted in minimum cutting force of 71 N, with the feed rate being the most significant factor followed by depth of cut and cutting speed. Therefore, it can be concluded that the simulation results can be considered in the machinability study of S45C material because this method saves the actual machining cost, and the results are reliable.

Received 15 August 2023; received in revised form 27 October 2023; accepted 7 January 2024.
To cite this article: Ghani et al., (2024). Machining analysis of S45C carbon steel using finite element method. Jurnal Tribologi 40, pp.226-246.

1.0 INTRODUCTION

Most countries around the world, including Malaysia, have already implemented Industrial Revolution 4.0 over the past few decades, where this phase refers to connectivity, automation, machine learning and real-time data. In other words, IR4.0 can also be defined as an intelligent manufacturing because of the combination of physical production with machine learning, intelligent digital technology, and big data. Among the activities involved in physical production as intended include the machining process. According to Kim et al., (2018), machine learning can be used in machining operations to improve product quality and productivity, monitor system health, and optimize design and process parameters. The machining process is known as a prototyping, and manufacturing technique that involves removing unwanted material from a larger material to obtain the desired shape. Referring to the description above, the machining process can also be considered as subtractive manufacturing following the process of building a part because of removing material from the work material (SYNECTIC, 2019).

The machining process is generally divided into two categories, namely conventional machining, and non-conventional machining. The difference that can be seen between these two categories of machining is the physical tools that must always be present in conventional machining operations such as single point cutting tool in lathes (Engineering, 2020), while in non-conventional machining it is the opposite. Examples of conventional machining that often stand out are lathes and drills (Kim et al., 2018). Examples of non-conventional machining are electrochemical machining (ECM), laser beam machining (LBM) and electrical discharge machining (EDM) (Oke et al., 2020). According to Oke et al. (2020), since there are difficulties in conventional machining involving cutting tool, non-conventional machining has attracted a lot of attention. Sustainability issues are also emphasized nowadays such as machining using cryogenic cooling (Halim et al., 2019).

Finite element method (FEM) is a numerical approach to perform finite element analysis (FEA) on any physical phenomenon. To fully understand and measure any physical phenomenon, such as structural or fluid behavior, heat transfer, wave propagation, and biological cell growth, mathematical solutions are required. Partial differential equations (PDEs) are used to describe most of these processes. Numerical algorithms have been developed over the past few decades to allow computers to solve these algorithms, and one of the most popular todays is the finite element method. In the past, the need to study complex structures in aviation engineering and the availability of electronic computers provided the real impetus for the creation of what is now known as the finite element approach (Bathe, 2008). Now there are many FEM applications that can be seen in various aspects including in terms of heat and fluid flow, biomedical applications, plate dynamics, animation, and computer visualization etc. (Rao et al., 2012). If viewed from a machining point of view, according to Kumar et al., (2016), the finite element method is one of the most used methods to calculate the stress, strain, displacement, shear stress, and temperature distribution in the cutting zone. Compared to actual testing techniques, FEM-based methods save time and materials, and can provide accurate estimates of chip formation, and workpiece temperatures during turning process.

The finite element method (FEM) has been widely used to simulate and predict various parts of the metal cutting process (Nasr & Ammar, 2017). This includes during the hard machining process (Guo & Yen, 2004), and cryogenic machining (Salame et al., 2019). Other aspects that use FEM are for the estimation of wear of the cutting tool (Malakizadi et al., 2016), the machining of long fiber composite models for aeronautical components (Santiuste et al., 2010), the study of plastic strain and plastic strain rate (Davim & Maranhão, 2009), as well as fiber reinforced plastic

(FRP) composite machining (Mkaddem et al., 2008). Study by Maity & Pradhan, (2018) on the machining of titanium alloy was applying a FEM DEFORM-3D software for analyzing the simulation of the micro-groove cutting inserts and the workpiece. Cutting temperature is one of the parameters that can be measured during the simulation process. The results of the study found that the percentage of error between simulation and experiment was only around four percent. This means that the use of FEM is able to provide accurate results that are equivalent to experiments. A study by Ma et al., (2016) also applied AdvantEdge FEM to evaluate the performance of micro hole textured cutting tool in dry machining of Ti-6Al-4V. The study utilizes adaptive mesh techniques and updated Langragian finite elements, along with continuous mesh to achieve the desired objective. Both the workpiece and the tool point were modelled using the same software.

The use of FEM applications other than AdvantEdge and DEFORM-3D, namely ABAQUS CAE can be seen through a study by Eltaggaz et al., (2020). The FEM equation used in this study is equation (1), where according to Eltaggaz et al., (2020) accurate pressure flow calculations to represent thermal behavior are very important since plastic deformation will factor into any temperature increase. Based on equation (1) $\boldsymbol{\rho}$ refers to the density of the material, $\boldsymbol{T}$ is the temperature rate while $\boldsymbol{\eta}$ is the inelastic heat fraction.

$$\boldsymbol{\rho}.\boldsymbol{c}(\boldsymbol{T}).\dot{\boldsymbol{T}} = \boldsymbol{\eta}.\boldsymbol{\sigma}.\dot{\boldsymbol{\varepsilon}}^{\boldsymbol{pl}} \tag{1}$$

In addition, two other equations which are equations (2) and (3) also play an important role according to Eltaggaz et al., (2020) because equation (2) helps in deducing the stress flow as a function of strain and strain force as well as temperature. While for equation (3) refers to the heat softening during the cutting process produced which is represented by $\boldsymbol{\psi(T)}$.

$$\boldsymbol{\sigma}(\boldsymbol{\varepsilon},\dot{\boldsymbol{\varepsilon}},\boldsymbol{T}) = (\boldsymbol{K_1} + \boldsymbol{K}.\boldsymbol{\varepsilon}^{\boldsymbol{n}} + \boldsymbol{\eta}.\dot{\boldsymbol{\varepsilon}}).\boldsymbol{\psi}(\boldsymbol{T}).\boldsymbol{\chi}(\boldsymbol{\varepsilon},\dot{\boldsymbol{\varepsilon}},\boldsymbol{T}) \tag{2}$$

$$\boldsymbol{\psi}(\boldsymbol{T}) = e^{\frac{-\beta.(T-T0)}{Tm}} \tag{3}$$

S45C is a carbon steel that has a moderate level of strength which is widely used for automotive parts, and for fabrication of various items such as line shafts, pins and gears. This material is also suitable for fabrication work such as locks and is usually produced as a nozzle structure in the oil and gas industry (Rifai et al., 2016). Study done by Shah et al., (2018) stated that S45C work material was selected because it has good strength, good machinability level and acceptable weldability. However according to Rifai et al., (2016), only a few literature studies have been conducted on machining experiments using S45C steel. Therefore, a comprehensive analysis as well as optimization and modelling are required to evaluate the metal machining performance of JIS S45C. Based on the research that has been done, since JIS S45C grade steel contains hard components such as chromium and silicon, the abrasion wear mode is prominent (Rifai et al., 2016). In another study, it was found that if the machining of carbon steel S45C is carried out at a high cutting speed, then the wet machining method is the best to produce a good quality surface (Yap et al., 2015). In addition, the drilling process carried out on the S45C showed the depth of cut to be the largest contributor to the heat generated, apart from the cutting speed and the feed rate (Shah et al., 2018). Ghani et al., (2017)found that the depth of cut has a greater impact than

the feed rate in determining the shear angle, where a large shear angle value can provide benefits such as low cutting temperature during the machining of S45C carbon steel. In addition, machining S45C at a low cutting speed will cause the formation of a large built-up edge size (BUE) (Song et al., 2017).

The focus of this study is to study the cutting parameters that affect the cutting force and resulting stress by using the FEM Abaqus CAE method for the range of cutting parameters commonly used in the industry in the machining of S45C carbon steel.

2.0 METHODOLOGY

The geometry of the cutting tool that will be used in the simulation is shown in Figure 1 according to DNMG150608N-SE, this cutting tool has a diamond shape with an angle of 55 degrees. A list of the geometry characteristics of the carbide tool tip used can be referred to in Table 1. The geometry of the tool tip used is produced through 2-Dimensional drawing on the software Abaqus CAE.

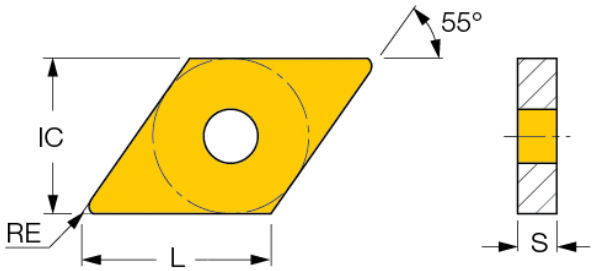

Figure 1: Schematic diagram of the cutting tool DNMG (Source: Hochleistungs-Zerspanungswerkzeuge et al., 2020).

The finite element software used is Abaqus CAE to build the machining model and the work material is carbon steel S45C. The carbide cutting tool geometry is in Figure 1 for the simulation of the orthogonal cutting. This simulation aims to identify the cutting parameters that affect the machining output of cutting force and stress in the machining of S45C workpieces.

Among the important parameters that are considered to ensure the accuracy and effectiveness of the simulation include the geometry of the cutting tool, the physical properties of the S45C workpiece and the carbide cutting tool as well as the Johnson-Cook material constant for the S45C carbon steel obtained from previous studies. The cutting tool geometry is listed in Table 1.

Table 1: Cutting tool geometry.

Geometry	**Value**
Rake angle (°)	-5
Clearance angle (°)	0
Nose radius (mm)	0.8

Based on the study by Kumar et al., (2016), the cutting tool used in the simulation is modelled as an elastic material where density, Poisson's ratio and isotropic conductivity are among the

parameters considered. This is because the physical properties found in the work material play a significant role in the formation of fragments. The fragments formed during the simulation are free to flow or break according to their physical properties and are affected by temperature, stress, and shape changes. The physical properties of S45C carbon steel and cutting tool are listed in Table 2.

Table 2: Mechanical properties of S45C work materials and carbide tool points.

Mechanical Properties	**Carbon Steel S45C**	**Carbide Cutting Tool**
Density (kg/m^3)	7700	11900
Young's Modulus (Gpa)	190	534
Poisson ratio	0.27	0.22
Thermal Conductivity (W / m °C)	49.8	40
Heat Capacity (J/Kg °C)	432.6	-

This simulation also apply the Johnson-Cook (J-C) constitutive equation combined with damage criteria in generating the formation of fragments as in the study by Jomaa et al., (2017). This material model is very reliable and has been proven useful in characterizing various material's behavior such as strains, strain rates and temperatures during the machining process even though it is a challenging process (Shrot & Bäker, 2011). The application of this model during FEM simulation can be seen in the study by Duan et al., (2009) and Jomaa et al., (2017) in analyzing at the temperature field distribution during the machining process. Therefore, the same model will be used in this study. The values of the Johnson-Cook parameters used to simulate the behavior of S45C carbon steel workpieces are shown in Table 3.

Table 3: Johnson-Cook parameter for S45C.

A (Mpa)	**B (Mpa)**	**n**	**C**	**m**	**$\dot{\varepsilon}_0$ (s^{-1})**	**T_m (°C)**	**T_0 (°C)**
553	600	0.234	0.0134	1	0.001	1460	20

The separation of fragments from the workpiece was simulated using the Johnson-cook damage model, where it is the most appropriate model for deformation at high strain rates (Sulaiman et al., 2014). The damage criteria calculated for each element in the model is by using equation (4).

$$\boldsymbol{D} = \boldsymbol{\Sigma} \left(\frac{\Delta \boldsymbol{\varepsilon}^{\boldsymbol{pl}}}{\boldsymbol{\varepsilon}_{\boldsymbol{f}}^{\boldsymbol{pl}}}\right. \tag{4}$$

The Johnson-Cook dynamic failure model used to determine failure parameters is using equation (5).

$$\boldsymbol{\varepsilon}_{\boldsymbol{f}}^{\boldsymbol{pl}} = \left[\boldsymbol{d_1} + \boldsymbol{d_2}\ \boldsymbol{exp}\ \left(\boldsymbol{d_3}\frac{\boldsymbol{p}}{\boldsymbol{q}}\right)\right]\left[\mathbf{1} + \boldsymbol{d_4}\ \boldsymbol{ln}\ \left(\frac{\boldsymbol{\varepsilon}^{\boldsymbol{pl}}}{\boldsymbol{\varepsilon_0}}\right)\right][\mathbf{1} + \boldsymbol{d_5}\frac{\boldsymbol{T}-\boldsymbol{T_0}}{\boldsymbol{T_{melt}}-\boldsymbol{T_0}} \tag{5}$$

Table 4 shows the Johnson-cook damage parameters for the S45C workpiece.

Table 4: Damage parameter for Johnson-Cook for S45C.

Damage Parameter	Specific value
Initial failure stress, d_1	0.06
Exsponen factor, d_2	3.31
Triaxsility factor, d_3	-1.96
Strain flow factor, d_4	0.0018
Suhu factor, d_5	0.58

2.1 Design of Experiment (DOE) For the Simulation

Table 5 summarizes in detail the experimental design (DOE) that will be carried out in this study where there are three different levels of simulation in terms of cutting speed, feed rate and depth of cut that are commonly used in industry and past researchers. Taguchi method of L9 orthogonal arry has been applied for the factors and levels in Table 5 to carry out all the simulation as in Table 6.

Table 5: Factors and level used in the simulation.

Factor/Level	1	2	3
Cutting Speed (mm/min)	160	200	240
Feed rate (mm/rev)	0.1	0.2	0.4
Depth of Cut (mm)	0.15	0.25	0.35

Table 6: Simulation trial for the study.

No.	Cutting Speed (m/min)	Feed Rate (mm/rev)	Depth of Cut (mm)
1	160	0.1	0.15
2	160	0.2	0.25
3	160	0.4	0.35
4	200	0.1	0.25
5	200	0.2	0.35
6	200	0.4	0.15
7	240	0.1	0.35
8	240	0.2	0.15
9	240	0.4	0.25

2.2 Modeling of The Cutting Tools and Work Materials

The length of the workpiece has been set to 2 mm, the height is divided into two i.e. 0.7 mm for the thickness from the bottom of the workpiece, and the thickness of the part that have not been formed is based on the feed rate (0.1mm - 0.4 mm). A dividing line with a size of 0.5 mm was introduced on the workpiece to help produce a denser and finer mesh on the fragment to improve

the accuracy of the results obtained. The cutting tool point for this simulation is drawn with a height of 1mm and has a pitch angle of -5° and a clearance angle of 0°.

The assembly of both cutting tool point and workpiece is arranged as on Figure 2 in which there is a slight clearance between the cutting tool point and workpiece. According to Soliman et al., (2020), this will avoid any inertial reaction that may occur between the cutting tool point and the workpiece before any movement begins and at the same time cause distortion of the workpiece mesh to occur.

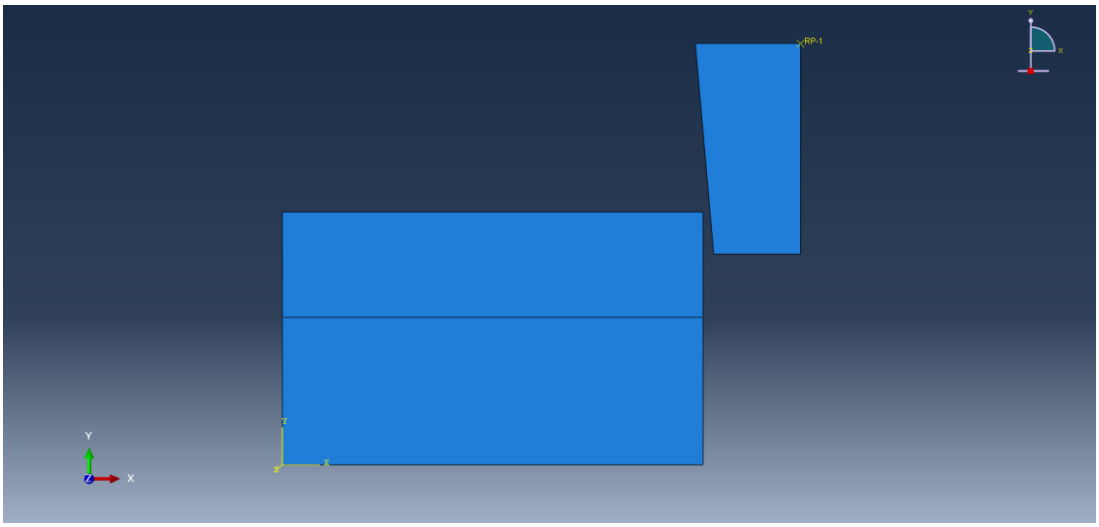

Figure 2: Model arrangement for S45C workpiece and cutting tool point.

2.3 Meshing for The Model

The meshing process on workpiece and tool point uses a 4-node bilinear, quadrilateral, reduced integration and automatic hourglass control element type (CPE4RT) elements. The mesh on the part of the fragment to be formed has a higher density than at the bottom of the workpiece. Figure 3 shows the mesh on the workpiece and the cutting tool point.

2.4 Turning Experiment

For validation purposes, a turning S45C was conducted at a cutting speed of 200 m/min, a feed rate of 0.2 mm/rev and depth of cut of 0.25 mm. This parameter was selected because it was used in industry for finishing process for material S45C (motorcycle shaft).

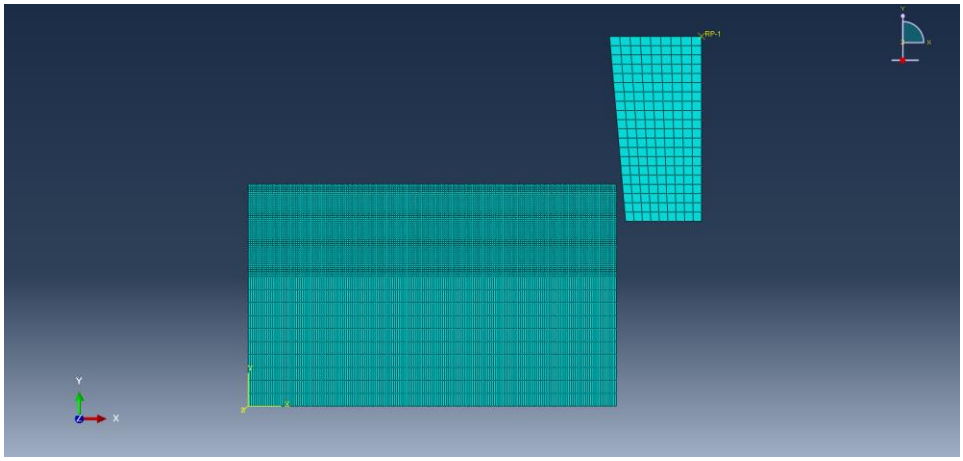

Figure 3: Meshing on the material and cutting tool.

3.0 RESULTS AND DISCUSSION

The simulation results discussed are cutting force, stress, and chip formation. To obtain these results, only one model was used for all the nine simulations, which is the Dynamic/Explicit analysis model. A total of ten experiments were carried out with nine experiments according to the input parameters as listed in Table 6, while one experiment was based on the machining parameter used by the industry, which is a cutting speed of 200 m/min, a feed rate of 0.2 mm/rev and a depth of cut of 0.25 mm. This is because the cutting force was measured experimentally at this machining condition which can be compared with the simulation results. Therefore, the 2-Dimensional orthogonal cutting model used in this study will be verified and if the error is small, it can be used for other materials in the future.

3.1 Cutting Force

Based on the simulation results, analysis of the factors that affect the cutting force generated has been done using the Taguchi method. The simulation data for the cutting force is shown in Table 7 while Figure 4 shows the cutting force obtained as well as the experiments that have been carried out.

Referring to Figure 4, the cutting force shows an increasing trend if the cutting speed is increased from 160 m/min up to 240 m/min at all feed rate values. This is because the increase in temperature in the cutting zone is not high enough to soften the machined material that could reduce the force required to cut the material. Chen et al., (2018) stated that the time for the heat dissipation of the work material to the environment is insufficient, then it contributes to the softening of the material due to the high temperature. This phenomenon does not occur in this study.

Referring to Table 7, only at a cutting speed of 160 m/min, the highest cutting force was observed due to the high value of the feed rate and depth of cut, resulting in high volume of the material to be cut. According to Ghoreishi et al., (2018), due to the thickness profile of the formed chip getting thicker in addition to the resistance that exists between the cutting tool and the workpiece during the machining process. Therefore, higher the cutting force was required to cut the workpiece.

Analysis using the Taguchi method was performed to identify and determine the optimal machining parameters, namely cutting speed (m/min), feed rate (mm/rev) and depth of cut (mm) to the cutting force in machining S45C workpieces. The smaller is better criterion was used in this study because a smaller force indicates better machinability. Tables 8 and 9 show the response for the signal to noise ratio and the average (Mean of Mean) for this simulation.

Table 7: Simulation results for the cutting force.

No.	Cutting Speed (m/min)	Feed Rate (mm/rev)	Depth of Cut (mm)	Cutting Force (N)
1	160	0.1	0.15	71.0515
2	160	0.2	0.25	181.252
3	160	0.4	0.35	406.261
4	200	0.1	0.25	134.822
5	200	0.2	0.35	283.935
6	200	0.4	0.15	188.714
7	240	0.1	0.35	188.994
8	240	0.2	0.15	122.545
9	240	0.4	0.25	328.850

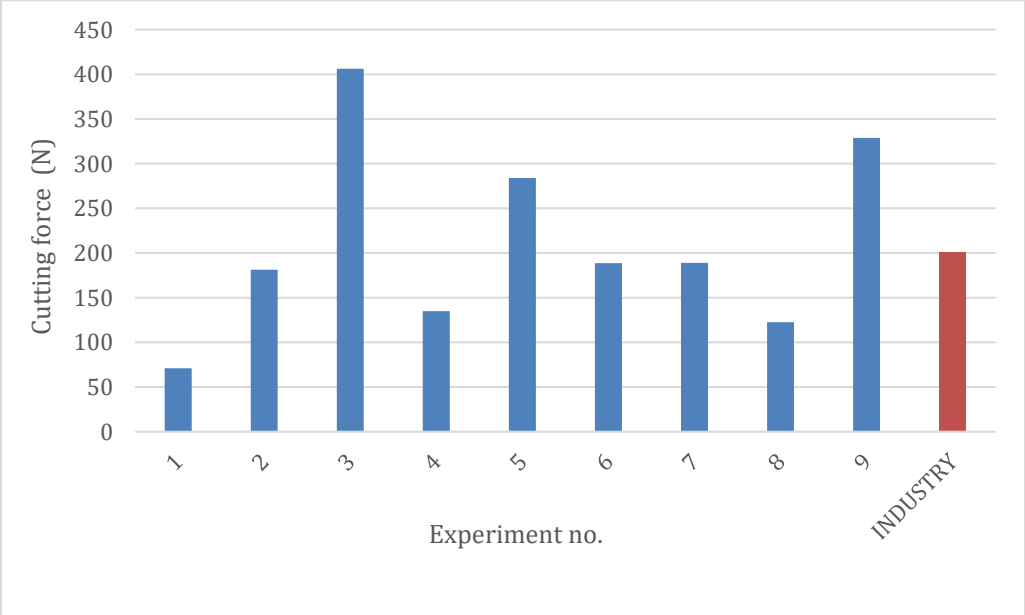

Figure 4: Cutting force for the simulation carried out.

Table 8: Respond table for signal to noise ratio.

Level	Cutting Speed (m/min)	Feed rate (mm/rev)	Depth of cut (mm)
1	-44.79	-41.72	-41.44
2	-45.73	-45.33	-46.03
3	-45.88	-49.34	-48.92
Delta	1.09	7.63	7.49
Rank	3	1	2

Table 9: Respond table for Mean of Mean.

Level	Cutting Speed (m/min)	Feed rate (mm/rev)	Depth of cut (mm)
1	219.5	131.6	127.4
2	202.5	195.9	215.0
3	213.5	307.9	293.1
Delta	17.0	176.3	165.6
Rank	3	1	2

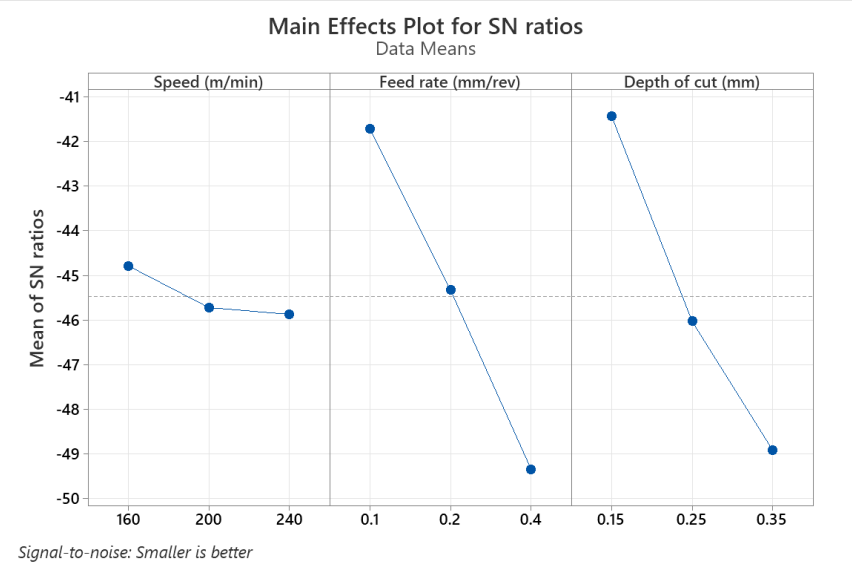

Figure 5: S/N plot for cutting force.

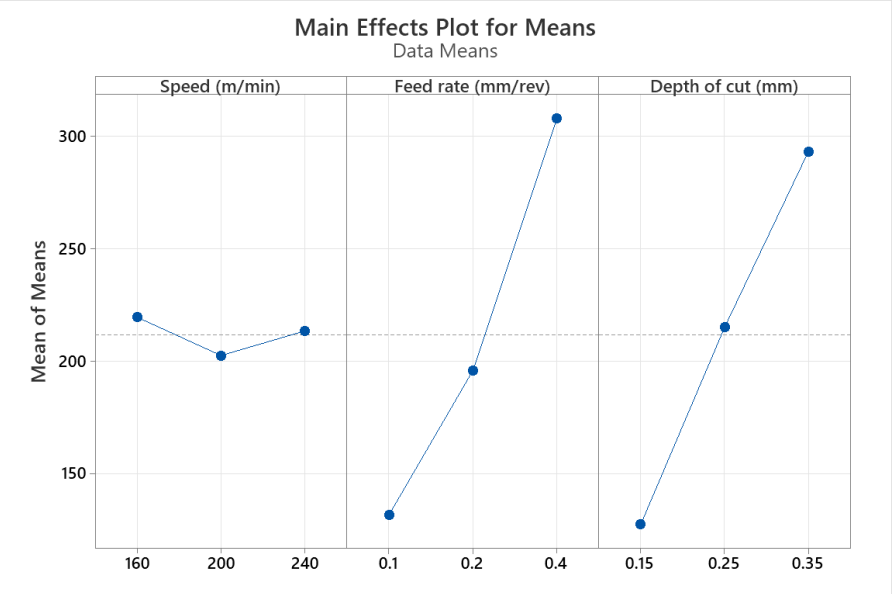

Figure 6: Mean plot for cutting force.

Figure 5 and Figure 6 show the plot of the signal to noise ratio and the average (Mean of Mean) for the cutting force. Based on Figure 5, feed rate has a significant effect on cutting force followed by cutting depth and cutting speed. Referring to Figure 5, the signal to noise ratio found that the optimal machining conditions for the S45C workpiece is at a speed of 160 m/min, depth of cut of 0.15 mm and a feed rate of 0.1 mm/rev. Optimum conditions are important during machining in order to achieve results with the desired quality.

3.2 Stress

Table 10 shows the stress output on the work material obtained during the simulation of the S45C material. It was found that high stress occurs at low levels for all cutting parameters, while at high levels of cutting speed, the stress is low. This agrees with the relationship between force and stress ($\sigma=F/A$), i.e. at high cutting speed, force will decrease, and A will increase at high depth and feed.

The S45C workpiece undergoes significant deformation during the chip formation process during machining simulations. Figure 7 shows the stress distribution recorded in experiment 8 where an uneven shear zone begins to form as soon as the tip of the tool comes into contact with the workpiece In Figure 8, the main shear zone begins to form after the tool point moves further towards the workpiece. The maximum value of the recorded stress is 1.416 GPa located in the main shear zone during this machining.

Table 10: Simulation results for the stress.

No.	Cutting speed (m/min)	Feed rate (mm/pusingan)	Depth of cut (mm)	Stress (GPa)
1	160	0.1	0.15	1.66477
2	160	0.2	0.25	1.61424
3	160	0.4	0.35	1.48393
4	200	0.1	0.25	1.48536
5	200	0.2	0.35	1.48822
6	200	0.4	0.15	1.41673
7	240	0.1	0.35	1.55704
8	240	0.2	0.15	1.41555
9	240	0.4	0.25	1.38446

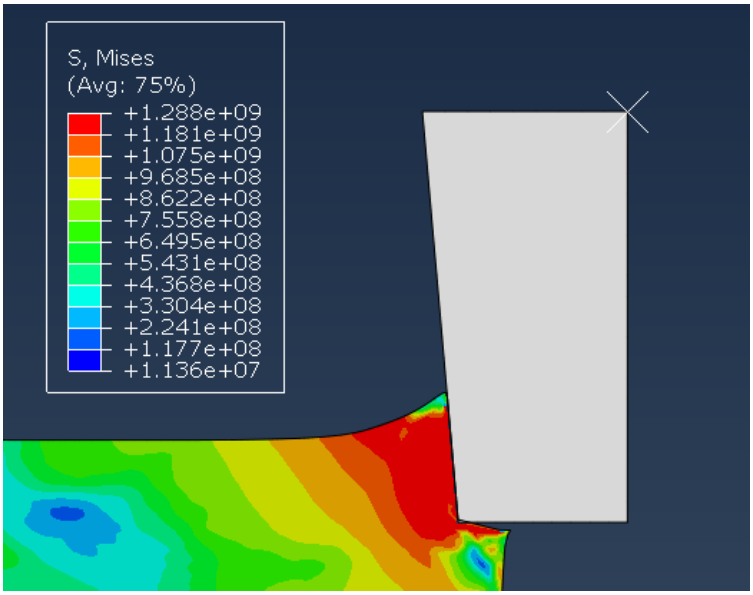

Figure 7: Formation of irregular shear zone.

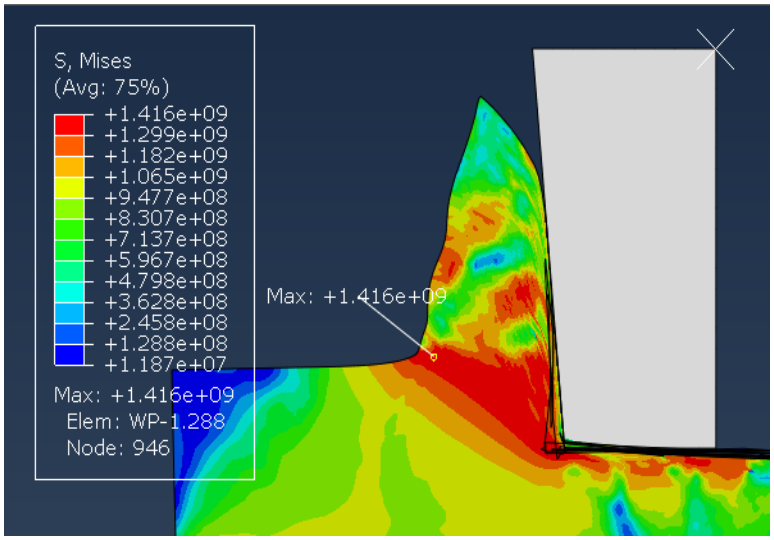

Figure 8: Formation of primary shear zone.

Table 11: Response table for signal to noise ratio.

Level	Cutting Speed (m/min)	Feed Rate (mm/rev)	Depth of Cut (mm)
1	-184.0	-183.9	-183.5
2	-183.3	-183.5	-183.5
3	-183.2	-183.1	-183.6
Delta	0.8	0.8	0.1
Ranking	2	1	3

Table 12: Response table for Mean of Mean.

Level	Cutting Speed (m/min)	Feed Rate (mm/rev)	Depth of Cut (mm)
1	1587646667	1569056667	1499016667
2	1463436667	1506003333	1494686667
3	1452350000	1428373333	1509730000
Delta	135296667	140683333	15043333
Ranking	2	1	3

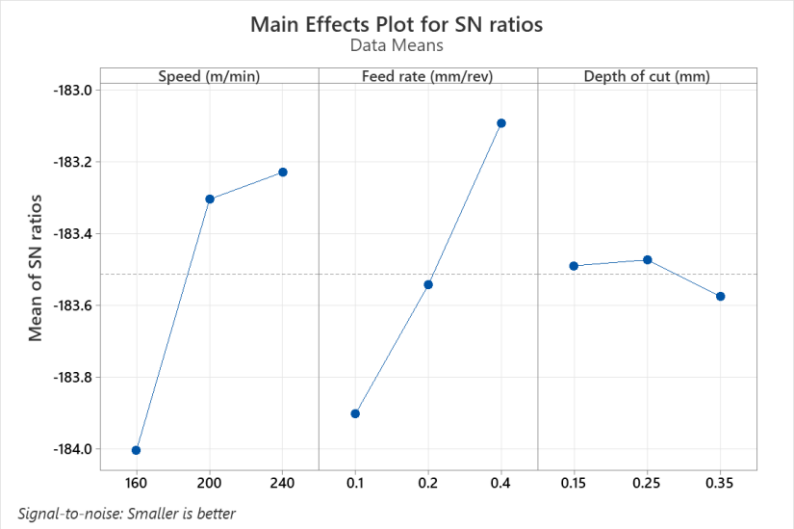

Figure 9: Signal to noise plot of stress.

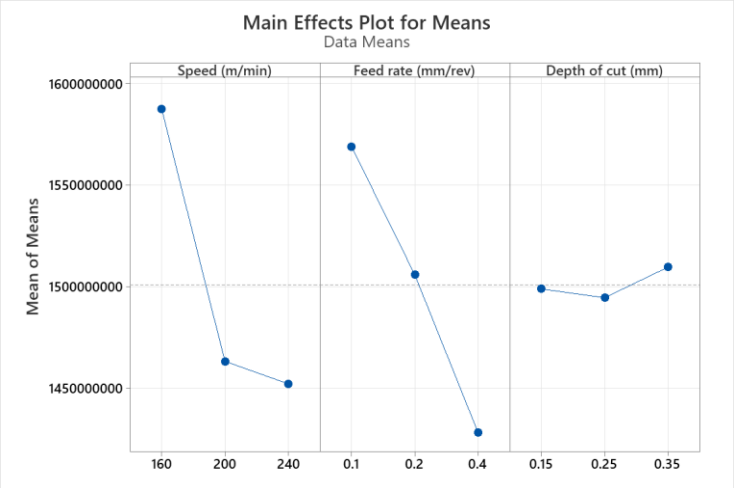

Figure 10: Mean plot for stress.

The Taguchi method (criterion: Smaller is better) is used for analysis the stress output. Table 11 and Figure 9 show that the feed rate is the factor that has the highest impact on the resulting stress followed by cutting speed and feed rate. Referring to Figure 9, the optimal parameters are at a cutting speed of 240 m/min, a feed rate of 0.4 mm/rev, and a cutting depth of 0.25 mm.

3.3 Comparison of Simulation Results of Cutting Force With Experiments

Comparison of the results obtained through simulation with experiments is important and should be done. This is to ensure that the simulation model used in the Abaqus CAE software is able to provide accurate, precise and reliable results by making estimates for various and complex machining parameters (Thasana & Chianrabutra, 2019). Many studies on various machining that also use Abaqus CAE software can be seen doing this comparison such as the study by Ducobu et

al., (2017), Vasu et al., (2021) and Thekdi, (2019). Various outputs can be used for comparison such as temperature, strain, and morphology of the formed chips. For this study, the comparison will be focused on the cutting force.

A comparison of the cutting force is made according to the industrial parameters used in the experimental method which is at a cutting speed of 200 m/min, a feed rate of 0.2 mm/rev and depth of cut of 0.25 mm. Table 13 shows these results.

Table 13: Cutting force results between experiment and simulation.

Results	Experiment	Simulation	Error (%)
Cutting force (N)	-211.603	200.671	5.2

Referring to Table 13, the percentage of error that can be observed is very low which is 5.2% indicating that this simulation model can be used to see more other outputs during the machining of S45C workpieces such as temperature, strain and tool wear.

3.4 The Relationships of The Cutting Force, Surface Roughness and Flank Wear In The Turning Experiment

The results in Table 13 indicates an acceptable results of the simulation and experimental results for industrial machining parameter at a cutting speed of 200 m/min, a feed rate of 0.2 mm/rev and depth of cut of 0.25 mm. Therefore a thorough analysis was carried experimentally out to seek the relationship of the cutting force, surface roughness and flank wear. Table 13 shows the results of the cutting force, surface roughness and flank wear at this industrial machining parameter.

Results in Table 14 shows that the Vb increases with cutting time until it reaches 0.3 mm which takes 119.00 minutes. The Vb is limited to 0.3 mm as specified in the standard for tool-life testing for turning process (ISO 3685 1977). By referring to the Vb, it was observed that the Ra values, and the cutting forces in Fx, Fy, and Fz directions increases with the values of Vb. The Ra values obtained is between 1.3 – 2.9 μm for fresh sharp tool until the edge of the cutting tool worn out at Vb = 0.3 mm.

Figure 11 (a)-(c) show the relationships between the resultant force and Vb, Ra and Vb, and Ra and Vb. These figures show that the resultant forces and Ra increase with Vb. Whereas Ra also increases with resultant forces. Therefore it can be concluded that the resultant force measured can be used as a reference to indicate the tool wear which is responsible to deteriorate the Ra values for the machined parts.

Table 14: Results of cutting time, flank wear, surface roughness and measured cutting forces in turning S45C at a cutting speed of 200 m/min, a feed rate of 0.2 mm/rev and depth of cut of 0.25 mm.

Trial run	Cutting time (min)	Flank wear, Vb (mm)	Surface roughness, Ra (μm)	Cutting force (N)			
				F_X	F_Y	F_Z	Resultant Force
1	0.28	0.000	0.000	216.150	156.257	132.047	297.61
2	5.67	0.046	1.275	204.949	138.360	120.163	274.93
3	11.33	0.065	2.150	184.193	116.813	103.011	241.21
4	17.00	0.076	1.796	214.156	171.025	131.853	304.13
5	22.67	0.081	2.122	184.523	122.812	106.631	245.97
6	28.33	0.083	2.504	183.184	120.044	107.094	243.80
7	39.67	0.085	2.077	191.052	135.192	112.280	259.59
8	51.00	0.188	2.835	207.968	162.537	137.446	297.59
9	53.83	0.194	2.303	207.609	170.775	140.537	303.34
10	56.67	0.203	2.505	217.145	165.352	142.683	307.98
11	59.50	0.210	2.575	218.767	165.427	146.845	311.11
12	62.33	0.212	2.746	217.603	177.785	149.667	318.37
13	68.00	0.221	1.336	226.878	183.256	154.385	329.99
14	73.67	0.231	1.706	233.895	214.872	163.497	357.22
15	77.35	0.233	1.716	232.749	184.484	159.386	337.06
16	79.33	0.233	2.174	223.505	203.183	159.370	341.52
17	85.00	0.238	2.091	227.101	192.812	162.099	339.16
18	90.67	0.244	1.619	244.120	235.198	184.405	385.90
19	96.33	0.254	2.060	231.413	211.930	170.085	356.92
20	102.00	0.267	2.367	231.499	196.841	163.829	345.22
21	107.67	0.270	2.364	243.701	238.263	185.092	387.84
22	113.33	0.284	2.659	235.831	219.675	175.123	366.80
23	119.00	0.300	2.941	235.767	206.830	169.638	356.57

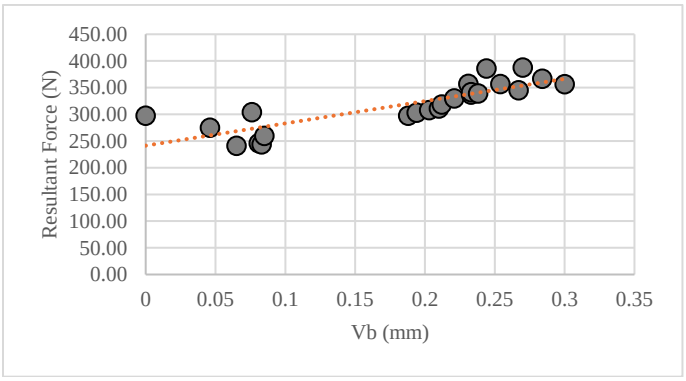

(a)

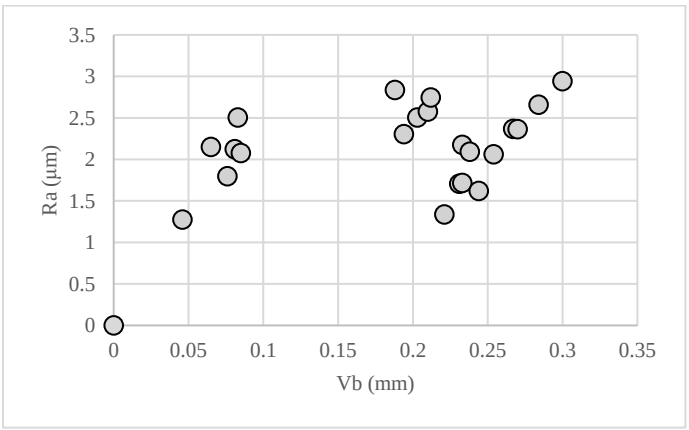

(b)

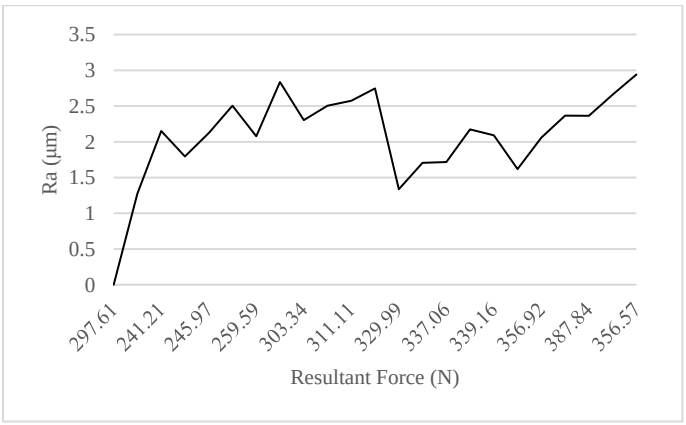

(c)

Figure 11: (a)-(c) the relationships between the resultant force and Vb, Ra and Vb, and Ra and Vb.

According to previous researcher (Araoyinboa et al., 2022), the surface roughness and other surface integrity in machining S45C can be improved by using cutting fluid. However, there was also contradicted finding (Yap et al., 2015) that found the machining in dry condition produced better surface roughness as compared in wet and cryogenic conditions. Therefore, it is important to find the optimum condition or the suitable range of machining parameters in order to have the desired results.

CONCLUSIONS

Cutting force and stress are affected by various machining parameters such as cutting speed, feed rate, and depth of cut. The cutting force increases as the feed rate and depth of cut increase but, will decrease if there is an increase in cutting speed due to material softening. However, the output value does not necessarily depend on only one parameter at a time, instead there are other cutting parameters that can affect the output.

Based on the range of cutting parameters, the lowest cutting force recorded throughout the simulation was 71.05 N. This value may be due to the three parameters used being at a minimum level. The highest cutting force value recorded was in experiment 3 which was 406.261 N. In this experiment, the cutting speed was the lowest, however, in cutting and the feed rate was at the highest level.

Based on the output that has been obtained and the application of the Taguchi method, this study succeeded in obtaining the optimal cutting parameters for the machining of S45C workpieces. The cutting parameters are a cutting speed of 160 m/min, a feed rate of 0.1 mm/rev and a cutting depth of 0.15 mm. This optimal machining condition will be able to help in improving the performance of the cutting tool during machining of S45C material.

The experimental results obtained indicates a good prediction of cutting force can be obtained using FEM simulation using sharp new cutting tool. However, when the tool progressively worn out, the cutting force increases with the flank wear land, which the main caused for the deterioration of the machined surface of the parts.

ACKNOWLEDGMENTS

The author would like to express his appreciation to the The Ministry of Higher Education and Universiti Kebangsaan Malaysia under grants GUP-2022-018 and FRGS/1/2019/TK03/UKM/01/2 for supporting this study.

REFERENCES

Araoyinboa, Oladeji, A., Edun, M. B., Samuel, A. U., Rahmat, A., Biodun, M. B., & Mustafa, M. A. (2022). Influence of Cutting Fluid on Machining Processes: A Review. *Jurnal Kejuruteraan*, *34(3)*, 365–373.

Bathe, K. J. (2008). Finite Element Method. In *Wiley Encyclopedia of Computer Science and Engineering* (pp. 1–12). John Wiley & Sons, Ltd. https://doi.org/doi:https://doi.org/10.1002/9780470050118.ecse159

Chen, Z., Peng, L., R., Z., J., R. M., Gustafsson, D., & Moverare, J. (2018). Effect of machining parameters on cutting force and surface integrity when high-speed turning AD 730TM with

PCBN tools. *The International Journal of Advanced Manufacturing Technology*, *100*, 2601–2615.
Davim, J. P., & Maranhão, C. (2009). A study of plastic strain and plastic strain rate in machining of steel AISI 1045 using FEM analysis. *Materials & Design*, *30(1)*, 160–165.
Duan, C., Cai, Y., Li, Y., & Wang, M. (2009). Finite element simulation of cutting temperature field during high speed machining hardened steel based on ABAQUS. *2009 2nd International Conference on Intelligent Computing Technology and Automation, ICICTA 2009*, *3*, 341–344. https://doi.org/10.1109/ICICTA.2009.549
Ducobu, F., Arrazola, P. J., Rivière-Lorphèvre, E., Zarate, G. O. De, Madariaga, A., & Filippi, E. (2017). The CEL Method as an Alternative to the Current Modelling Approaches for Ti6Al4V Orthogonal Cutting Simulation. *Procedia CIRP*, *58*, 245–250. https://doi.org/10.1016/j.procir.2017.03.188
Eltaggaz, A., Said, Z., & Deiab, I. (2020). An integrated numerical study for using minimum quantity lubrication (MQL) when machining austempered ductile iron (ADI). *International Journal on Interactive Design and Manufacturing*, *14*(3), 747–758. https://doi.org/10.1007/s12008-020-00662-z
Engineering, A. S. (2020). *The Difference Between Conventional and Non-Conventional Machining Process*. https://aerospeceng.com.au/the-difference-between-conventional-and-non-conventional-machining-process/
Ghani, J. A., Hassan, C., Haron, C., Othman, H., & Raof, N. A. (2017). Chip formation in turning S45C medium carbon steel in cryogenic conditions. *Jurnal Tribologi*, *14*(May), 1–9.
Ghoreishi, R., Roohi, A. H., & Dehghan Ghadikolaei, A. (2018). Analysis of the influence of cutting parameters on surface roughness and cutting forces in high speed face milling of Al/SiC MMC. *Materials Research Express*, *5*(8). https://doi.org/10.1088/2053-1591/aad164
Guo, Y. B., & Yen, D. W. (2004). A FEM study on mechanisms of discontinuous chip formation in hard machining. *Journal of Materials Processing Technology*, *155–156*(1–3), 1350–1356. https://doi.org/10.1016/j.jmatprotec.2004.04.210
Halim, N. H. A., Haron, C. H. C., Ghani, J. A., & Azhar, M. F. (2019). Tool wear and chip morphology in high-speed milling of hardened Inconel 718 under dry and cryogenic CO2 conditions. *WEAR*, *426*, 1683–1690.
Hochleistungs-Zerspanungswerkzeuge, G., Katalog, S., & Ogólny, K. (2020). *Performance Of Cutting Tools.*
Jomaa, W., Mechri, O., Lévesque, J., Songmene, V., Bocher, P., & Gakwaya, A. (2017). Finite element simulation and analysis of serrated chip formation during high–speed machining of AA7075–T651 alloy. *Journal of Manufacturing Processes*, *26*, 446–458. https://doi.org/10.1016/j.jmapro.2017.02.015
Kim, D. H., Kim, T. J. Y., Wang, X., Kim, M., Quan, Y. J., Oh, J. W., Min, S. H., Kim, H., Bhandari, B., Yang, I., & Ahn, S. H. (2018). Smart Machining Process Using Machine Learning: A Review and Perspective on Machining Industry. *International Journal of Precision Engineering and Manufacturing - Green Technology*, *5*(4), 555–568. https://doi.org/10.1007/s40684-018-0057-y
Kumar, B. V. R. M., Reddy, K. H., & Kumar, C. R. V. (2016). Finite element model based on abaqus / explicit to analyze the temperature effects of turning. *International Journal of Applied Engineering Research*, *11(8)*, 5728–5734.
Ma, J., Ge, X., Qiu, C., & Lei, S. (2016). FEM assessment of performance of microhole textured cutting tool in dry machining of Ti-6Al-4V. *International Journal of Advanced Manufacturing Technology*, *84*(9–12), 2609–2621. https://doi.org/10.1007/s00170-015-7918-0

Maity, K., & Pradhan, S. (2018). Investigation of FEM Simulation of Machining of Titanium Alloy Using Microgroove Cutting Insert. *Silicon*, *10*(5), 1949–1959. https://doi.org/10.1007/s12633-017-9707-x

Malakizadi, A., Gruber, H., Sadik, I., & Nyborg, L. (2016). An FEM-based approach for tool wear estimation in machining. *Wear*, *368–369*, 10–24. https://doi.org/10.1016/j.wear.2016.08.007

Mkaddem, A., Demirci, I., & Mansori, M. El. (2008). A micro-macro combined approach using FEM for modelling of machining of FRP composites: Cutting forces analysis. *Composites Science and Technology*, *68*(15–16), 3123–3127. https://doi.org/10.1016/j.compscitech.2008.07.009

Nasr, M. N. A., & Ammar, M. M. A. (2017). An Evaluation of Different Damage Models when Simulating the Cutting Process Using FEM. *Procedia CIRP*, *58*, 134–139. https://doi.org/10.1016/j.procir.2017.03.202

Oke, S. R., Ogunwande, G. S., Onifade, M., Aikulola, E., Adewale, E. D., Olawale, O. E., Ayodele, B. E., Mwema, F., Obiko, J., & Bodunrin, M. O. (2020). An overview of conventional and non-conventional techniques for machining of titanium alloys. *Manufacturing Review*, *7*. https://doi.org/10.1051/mfreview/2020029

Rao, M. A., Khanna, M. R., Somaiya, K. J., & Gangopadhyay, M. (2012). Applications of Finite Elements Method (FEM) - An Overview. *International Conference on Mathematical Sciences*, *28*(31), 1–8. https://doi.org/10.13140/RG.2.2.36294.42565

Rifai, D., Abdalla, A. N., Khamsah, N., Aizat, M., & Fadzli, M. (2016). Subsurface defects evaluation using eddy current testing. *Indian Journal of Science and Technology*, *9*(9). https://doi.org/10.17485/ijst/2016/v9i9/88724

Salame, C., Bejjani, R., & Marimuthu, P. (2019). A better understanding of cryogenic machining using CFD and FEM simulation. *Procedia CIRP*, *81*, 1071–1076. https://doi.org/10.1016/j.procir.2019.03.255

Santiuste, C., Soldani, X., & Miguélez, M. H. (2010). Machining FEM model of long fiber composites for aeronautical components. *Composite Structures*, *92*(3), 691–698. https://doi.org/10.1016/j.compstruct.2009.09.021

Shah, A. H. A., Hussain, S., & Asari, M. S. (2018). The effects of machining parameter on temperature changes in milling process for S45C carbon steel. *AIP Conference Proceedings*, *2030*. https://doi.org/10.1063/1.5066733

Shrot, A., & Bäker, M. (2011). How to identify johnson-cook parameters from machining simulations. *AIP Conference Proceedings*, *1353*(1), 29–34. https://doi.org/10.1063/1.3589487

Soliman, H. A., Shash, A. Y., El Hossainy, T. M., & Abd-Rabou, M. (2020). Investigation of process parameters in orthogonal cutting using finite element approaches. *Heliyon*, *6*(11), e05498. https://doi.org/10.1016/j.heliyon.2020.e05498

Song, X., Takahashi, Y., He, W., & Ihara, T. (2017). On the formation mechanisms of adhering layer during machining metal material. *Key Engineering Materials*, *749 KEM*, 39–45. https://doi.org/10.4028/www.scientific.net/KEM.749.39

Sulaiman, S., Roshan, A., & Borazjani, S. (2014). Effect of cutting parameters on tool-chip interface temperature in an orthogonal turning process. *Advanced Materials Research*, *903*, 21–26. https://doi.org/10.4028/www.scientific.net/AMR.903.21

SYNECTIC. (2019). *What is machining? A machining and CNC machining FAQ*. https://synectic.net/what-is-machining/

Thasana, W., & Chianrabutra, S. (2019). A comparison between simulation and experiment of virtual machining in CNC turning machine considering kinematic motion deviations, tool wear and workpiece deflection errors. *Journal of Advanced Mechanical Design, Systems and*

Manufacturing, *13*(1), 1–12. https://doi.org/10.1299/jamdsm.2019jamdsm0009

Thekdi, P. N. (2019). *FINITE ELEMENT STUDIES OF ORTHOGONAL MACHINING OF AISI 1045 STEEL*. The University of North Carolina at Charlotte.

Vasu, C., Thaware, A., Tiwari, G., & Dumpala, R. (2021). Experimental and numerical analysis of orthogonal cutting of high strength aluminium alloy Al7075-T6. *IOP Conference Series: Materials Science and Engineering*, *1185*(1), 012010. https://doi.org/10.1088/1757-899x/1185/1/012010

Yap, T. C., Sivaraos, A., Lim, C. S., & Leau, J. W. (2015). Surface roughness and cutting forces in cryogenic turning of carbon steel. *Journal of Engineering Science and Technology*, *10*(7), 911–920.